

Structure and Polymorphic Behavior of High Molecular Weight Poorly Syndiotactic Polypropylene

Claudio De Rosa,* Finizia Auriemma, and Odda Ruiz de Ballesteros

Dipartimento di Chimica, Università di Napoli "Federico II", Complesso Monte S. Angelo, Via Cintia, 80126 Napoli, Italy

Received June 13, 2003; Revised Manuscript Received November 4, 2003

ABSTRACT: An analysis of the structure and polymorphic behavior of high molecular weight, low stereoregular, poorly crystalline syndiotactic polypropylene (sam-PP), prepared with heterocycle-fused indenylsilylamidodimethyltitanium complexes is presented. The samples do not crystallize by cooling the melt to room temperature but slowly crystallize if they are kept at room temperature for several days. Disordered modifications of the helical form I of syndiotactic polypropylene (s-PP) are obtained, and small degrees of crystallinity (16–20%) are achieved. The stretching of compression-molded films of sam-PP samples produces oriented crystalline fibers in the *trans*-planar mesomorphic form of s-PP. The low stereoregularity ($[rrrr] = 40\text{--}55\%$) prevents the formation of the ordered *trans*-planar form III of s-PP, which instead is obtained in stretched fibers of the highly stereoregular and crystalline s-PP. The *trans*-planar mesomorphic form, in turn, transforms into the helical form I upon release of the tension in stretched fibers of sam-PP samples. The isochiral helical form II of s-PP, which is generally obtained in s-PP fibers initially in the *trans*-planar form III by removing the tension, has never been observed in the sam-PP fiber samples. These data confirm that the isochiral form II of s-PP can be obtained only starting from the *trans*-planar form III through a spontaneous cooperative crystal–crystal transformation when the tension in stretched fibers is removed.

Introduction

The synthesis and a preliminary characterization of high molecular weight, low syndiotactic, poorly crystalline polypropylene have been recently described.¹ The polymer samples have been prepared with catalytic systems composed of silyl-bridged indenyl-*tert*-butyl-amido complexes of titanium, in which the indenyl ligand has a heterocycle condensed onto the cyclopentadienyl moiety (Chart 1).^{2,3} The catalysts **1** and **2** (Chart 1), activated with methylaluminoxane (MAO), show high activity in propylene polymerization, producing polypropylene samples with high molecular weights,¹ and a prevalently syndiotactic microstructure, with fully syndiotactic pentad contents $[rrrr]$ in the range 40–55%. We have defined these samples *syndiotactic-amorphous* polypropylene (sam-PP).¹

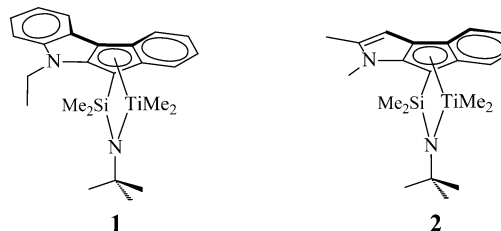
It is well-known that the stereoregularity of syndiotactic polypropylene (s-PP) strongly influences its polymorphism.^{4–8} A different polymorphic behavior is therefore expected for low stereoregular sam-PP samples.

The complex polymorphic behavior of s-PP has been extensively described,^{4–20} and clarified mainly through the analysis of highly crystalline and stereoregular s-PP prepared with the C_s -symmetric metallocene catalyst.^{4–7,12–15} Four different crystalline forms, shown in Figure 1, have been found.

The most stable form I (Figure 1A,B)¹² and the metastable form II (Figure 1C)¹⁰ are characterized by chains in $s(2/1)2$ helical conformation, packed in orthorhombic unit cells. The metastable form III (Figure 1D) presents chains in *trans*-planar conformation,¹⁶ whereas form IV (Figure 1E) is characterized by chains in $(T_6G_2T_2G_2)_n$ helical conformations.¹⁷

Besides the four crystalline forms, a disordered mesomorphic modification, characterized by chains in

Chart 1



trans-planar conformation packed in a disordered lattice, has also been obtained by quenching the melt at 0 °C and keeping the sample at 0 °C for a long time.^{21,22}

The formation of the four crystalline modifications depends on the condition of crystallization and the stereoregularity of the sample.^{4–8,12–15} Form I (Figure 1A,B) can be easily obtained by crystallization from the melt and from polymer solutions.^{12–15} Form II is characterized by a C-centered structure, where 2-fold helical chains having the same chirality are included in the orthorhombic unit cell (Figure 1C).¹⁰ It is a metastable polymorph of s-PP and has been obtained at atmospheric pressure only in oriented fibers of s-PP,^{4,6,10,20,23} for instance, by stretching at room temperature compression-molded specimens of low stereoregular s-PP samples prepared with vanadium-based Ziegler–Natta catalysts,^{4,6,10,20} or upon release of the tension in stretched fibers of highly stereoregular s-PP samples initially in form III,^{6,20,23} or, finally, by annealing fibers in form III.^{4,6} Recently, form II has been obtained also by melt crystallization at elevated pressure,²⁴ and by epitaxial crystallization of single crystals.²⁵ In powder unoriented s-PP samples only disordered modifications of form II, characterized by conformationally disordered chains containing *trans*-planar sequences (kink band defects),^{26–28} can be obtained at atmospheric pressure, for instance, by precipitation from solutions of low stereoregular samples,²⁶ and in copolymers of s-PP with ethylene comonomeric units.^{29–31}

* To whom correspondence should be addressed. Phone: ++39 081 674346. Fax: ++39 081 674090. E-mail: derosa@chemistry.unina.it.

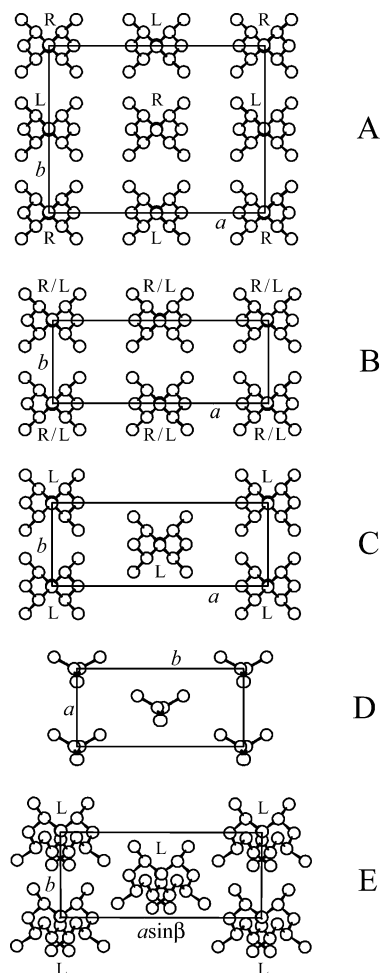


Figure 1. Models of packing of the limit-ordered form I (A), the limit-disordered form I (B), form II (C), form III (D), and form IV (E) of s-PP. R = right-handed helix, and L = left-handed helix.

The influence of the stereoregularity on the polymorphic behavior of s-PP has been studied through the characterization of samples prepared with the classic C_s -symmetric metallocene catalysts, having fully syndiotactic pentad contents $[rrrr]$ in the range 75–96%.^{5–8,20} As-prepared and melt-crystallized samples of s-PP having a high degree of stereoregularity (with $[rrrr]$ higher than 90%) always crystallize in the most stable form I.^{12–15,4,5,18} As shown in ref 5, form I of s-PP crystallizes from the melt in different modifications characterized by variable amounts of disorder depending on the crystallization temperatures. The limit-ordered modification of form I, characterized by a regular alternation of right- and left-handed 2-fold helical chains along both axes of the unit cell (Figure 1A),^{12,15} is obtained at high values of the crystallization temperature.^{12,5} For lower stereoregular samples, with $[rrrr]$ in the range 88–75%, disordered modifications of form I, characterized by disorder in the alternation of right- and left-handed helical chains along the axes of the units cell (Figure 1B), are always obtained by melt crystallization, even at high crystallization temperatures.^{6,7} In these samples, small amounts of crystals of form II (Figure 1C) are present⁶ and/or a mode of packing of form II occurs as a defect in a prevailing mode of packing of form I.⁷ This kind of defect corre-

sponds to a disorder in the stacking of *bc* layers of chains along the *a* axis, implying *b*/*4* shifts among consecutive *bc* layers piled along *a*.^{14,15,32} Less stereoregular samples are therefore not able to crystallize from the melt in the ordered form I owing to the tendency to form local arrangements of the chains as in form II.^{6,7}

Different polymorphic behaviors in samples having different stereoregularities have been observed also in oriented fibers.^{6,20} The pure *trans*-planar form III is, indeed, obtained only for highly syndiotactic samples ($[rrrr]$ higher than 90%) by stretching compression-molded films at room temperature,^{4,6,16,20} or by cold-drawing at temperatures below the glass transition temperature.^{4,11,16,33} The *trans*-planar form III generally transforms into the helical form II upon release of the tension.^{6,20,23} The lower the syndiotacticity, the more difficult the formation of the *trans*-planar form III by stretching.^{6,20} Lower stereoregular samples ($[rrrr] = 70$ –80%) give by stretching at moderate draw ratio fibers in mixtures of helical and *trans*-planar forms, and only at very high draw ratios the pure *trans*-planar form III is obtained.²⁰ The different polymorphic behavior upon stretching is most probably linked to the different amounts of defects of stereo- and regioregularity of the chains. It has been suggested that defects of stereoregularity and, probably, even regioregularity are highly tolerated within the lattices of the crystalline modifications of s-PP with chains in helical conformation,^{6,20,32} whereas such defects would be hardly included in the crystalline lattice of the *trans*-planar form III. The same reason can explain the experimental evidence that the pure *trans*-planar mesomorphic form can be obtained only for highly stereoregular s-PP samples, by quenching the melt at 0 °C and keeping the sample at 0 °C for a long time.⁸ In low stereoregular s-PP the crystallization of the stable helical form at room temperature is not completely inhibited even for long permanence time of the sample at 0 °C.⁸ In the presence of large amounts of configurational defects long portions of s-PP chain are able to crystallize only if they assume the helical conformation.

In this paper a structural characterization of poorly syndiotactic sam-PP samples is presented. This study may give new insights into the relationship between the microstructure of the polymer chains (amount of stereo-defects) and the structural organization of s-PP.

Experimental Section

Poorly syndiotactic sam-PP samples have been provided by Dr. Luigi Resconi of Basell Polyolefins (Ferrara, Italy). The samples have been prepared using the catalysts **1** and **2** (Chart 1) activated with MAO, as described in ref 1. The intrinsic viscosities, the molecular weights, the melting temperatures, and the microstructural characteristics (distribution of pentad stereosequences) are reported in Table 1. As described in ref 1, the samples sam-PP3, sam-PP4, and sam-PP5 have been obtained by performing the propylene polymerization with the catalyst **2**/MAO supported on polyethylene.

The NMR analysis indicates that all sam-PP samples present low syndiotacticity with concentrations of the fully syndiotactic pentad *rrrr* in the range 40–55%.

Amorphous specimens of the sam-PP samples have been obtained by compression molding of as-polymerized samples. Crystallization of the samples has been performed keeping the compression-molded specimens at room temperature for several days.

Oriented fibers of sam-PP samples have been obtained by stretching at room temperature and at a drawing rate of 10 mm/min of compression-molded samples after complete crys-

Table 1. Polymerization Temperatures (T_p), Intrinsic Viscosities (IV), Molecular Weights (M_w), Melting Temperatures (T_m), and Contents of Pentad and Diad Stereosequences (%) of sam-PP Samples Prepared with Catalysts 1 and 2/MAO

sample	T_r (°C)	catalyst	IV (dL/g)	M_w	T_m (°C)	[mmmm]	[mmmr]	[rmmr]	[mmrr]	[xmrx]	[rmm]	[rrrr]	[mrrm]	[mrrm]	[m]	[r]
sam-PP1	70	1	5.96	1308600	59	0.31	1.75	2.90	8.81	10.32	2.38	54.62	16.31	2.59	15.73	84.27
sam-PP2	60	2	3.65	672700	50	0.00	1.36	2.91	7.05	13.69	2.83	51.60	17.52	3.04	16.06	83.94
sam-PP3	80	2^a	5.43	1153200	48	0.53	2.01	3.24	7.73	14.81	3.84	45.84	18.64	3.36	18.97	81.03
sam-PP4	80	2^a	4.47	885700	48	0.27	2.14	3.39	7.55	13.76	3.66	46.86	18.02	4.35	18.29	81.72
sam-PP5	80	2^a	3.31	589200	47	0.78	2.69	3.75	8.84	15.63	4.64	41.42	18.33	3.92	21.77	78.23

^a Samples sam-PP3, sam-PP4 and sam-PP5 have been prepared with the catalyst 2/MAO supported on polyethylene.¹

tallization was achieved. Compression-molded films have been kept at room temperature for at least one week before stretching.

X-ray diffraction patterns were obtained with Ni-filtered Cu K α radiation. The powder profiles were obtained with an automatic Philips diffractometer, whereas the fiber diffraction patterns were recorded on a BAS-MS imaging plate (Fuji Film) using a cylindrical camera and processed with a digital imaging reader (FUJIBAS 1800). The X-ray fiber diffraction patterns have been recorded for stretched fibers soon after the stretching and keeping the fiber under tension, as well as for relaxed fibers, that is, after the fiber was kept under tension for 2 h and then the tension was removed, allowing the complete relaxation of the specimens. In the case of the stress-relaxed fibers, the diffraction patterns have been recorded 10 min after the release of the tension. All the X-ray fiber diffraction experiments have been performed with 2 h of exposure time. To make the crystalline Bragg reflections more visible, the X-ray diffraction pattern of the amorphous phase, obtained from the diffraction of atactic polypropylene, has been scaled for a suitable factor and subtracted from all the fiber diffraction patterns.

The melting temperatures were obtained with a differential scanning calorimeter, Perkin-Elmer DSC-7, performing scans in a flowing N₂ atmosphere and at a heating rate of 10 °C/min.

Results and Discussion

Unoriented Powder Samples. As-prepared sam-PP samples are generally amorphous. They do not crystallize by cooling the melt to room temperature, but slowly crystallize if the samples are kept at room temperature for several days. The X-ray powder diffraction profiles of the sample sam-PP1 cooled from the melt to room temperature and kept at room temperature for different times up to the complete crystallization are reported in Figure 2. Similar behavior has been observed for the other sam-PP samples of Table 1. All the samples crystallize in form I of s-PP (Figure 1A,B), as indicated by the presence in the X-ray diffraction profiles of Figure 2 of the 200 and 020 reflections at $2\theta = 12.2^\circ$ and 16° , respectively.

The diffraction patterns however indicate that disordered modifications of form I (Figure 1B) are obtained.⁵ The absence of the 211 reflection at $2\theta = 18.8^\circ$, typical of the ordered form I,¹² indicates that disorder in the alternation of right- and left-handed helical chains along the axes of the unit cell is present, whereas the presence of a broad peak in the range $2\theta = 13\text{--}19^\circ$, centered on the 020 reflection at $2\theta = 16^\circ$, indicates that a high amount of disorder in the stacking of *bc* layers of chains along *a*, implying shifts of *bc* layers of chains of *b*/4 along *b*, is also present.^{5,15,32} The latter kind of disorder produces local arrangements of the chains as in the C-centered form II of s-PP. A maximum crystallinity of nearly 18–20% is achieved for the two more syndiotactic sam-PP1 and sam-PP2 samples ([*rrrr*] = 50–55%), with melting temperatures of 59 and 50 °C, respectively. A lower crystallinity of nearly 16% is instead achieved for

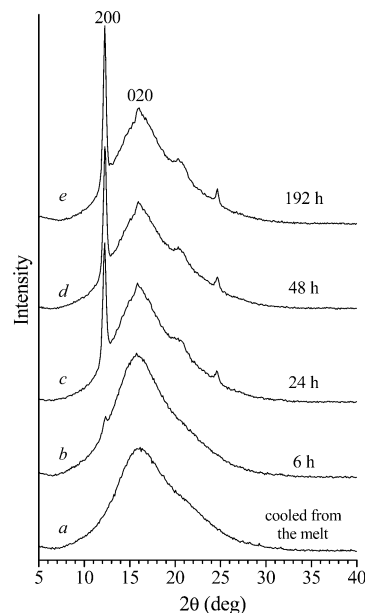


Figure 2. X-ray powder diffraction profiles of the sample sam-PP1 cooled from the melt and kept at room temperature for the indicated time. The 200 and 020 reflections at $2\theta = 12^\circ$ and 16° , respectively, of the helical form I of s-PP are indicated.

the lower syndiotactic samples sam-PP3–sam-PP5 ([*rrrr*] = 41–47%), with melting temperatures of 47–48 °C (Table 1).

Oriented Fiber. Oriented fibers of sam-PP samples have been obtained by stretching compression-molded films, after the complete crystallization in form I. The X-ray diffraction patterns of fibers of the sample sam-PP1 obtained by stretching at deformations ϵ of 100% and 300% are reported in parts A and B, respectively, of Figure 3. The presence of the 200 reflection at $2\theta = 12.2^\circ$ and of reflections on the first layer line corresponding to the periodicity of the helical conformation (7.4 Å) in the X-ray diffraction patterns of Figure 3 indicates that at low deformations (up to 300% strain) fibers in the helical forms of s-PP are obtained. Moreover, a broad halo of high intensity in the range $2\theta = 15\text{--}18^\circ$, corresponding to the scattering of the amorphous phase, is also present in the patterns of Figure 3. The presence of the large scattering due to the amorphous component prevents the recognition of the crystalline helical form present in these oriented fibers. In fact, the 020 reflection at $2\theta = 16^\circ$, typical of the helical form I, and the 110 reflection at $2\theta = 17^\circ$, typical of the helical form II, are hidden by the broad amorphous scattering (Figure 3).

It is apparent from Figure 3A that a low degree of orientation of the crystals of the helical form is obtained at 100% deformation. At higher deformation (300% strain) an increase of the degree of orientation of the crystalline phase is obtained, as indicated by the strong polarization of the 200 reflection at $2\theta = 12.2^\circ$ on the

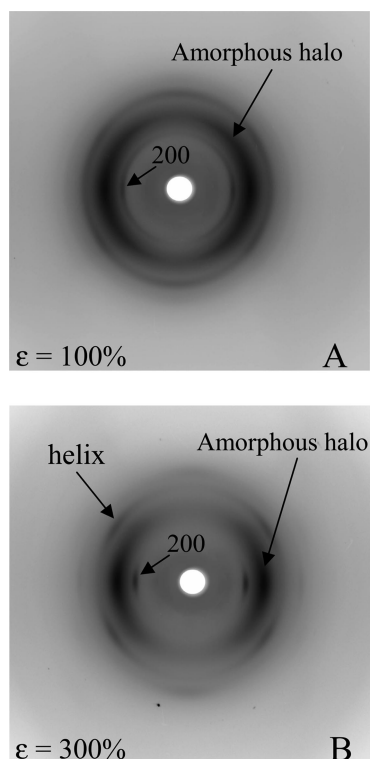


Figure 3. X-ray fiber diffraction patterns of fibers of the sample sam-PP1 obtained by stretching at room temperature compression-molded films at deformations ϵ of 100% (A) and 300% (B). The 200 reflection at $2\theta \approx 12^\circ$ typical of the helical forms of s-PP and the broad halo at $2\theta = 15\text{--}18^\circ$ arising from the scattering of the amorphous phase are indicated.

equator (Figure 3B). Moreover, with increasing deformation, also an increase of the polarization of the broad halo of the amorphous phase close to the equatorial line is observed (Figure 3B). In fact, it is apparent from Figure 3B that the intensity of the amorphous scattering

strongly decreases in the meridional region and appears more concentrated on the equator. This indicates that the stretching induces orientation of c axes of crystals of the helical form, as well as orientation of chains of the amorphous phase along the stretching direction. The amorphous chains probably assume more extended conformations upon stretching at high values of the deformation.

To better analyze the crystal forms which develop during the stretching, the scattering of the amorphous phase has been subtracted from the X-ray diffraction patterns. The X-ray fiber diffraction patterns of fiber specimens of the sample sam-PP1 obtained by stretching at different draw ratios, and keeping the fiber under tension, are reported in Figure 4, after the subtraction of the amorphous halo. The corresponding intensity profiles read along the equatorial line are also reported in Figure 4. Similar patterns have been obtained for the sample sam-PP2. It is apparent that the subtraction of the amorphous scattering allows recognition of the presence of the 020 reflection at $2\theta = 16^\circ$ of the helical form I in the X-ray diffraction patterns of Figure 4A,B. This indicates that for low deformations (up to $\epsilon \approx 300\%$) fibers in the helical form I are obtained. With increasing deformation the intensity of the 200 reflection at $2\theta = 12^\circ$ of the helical form decreases, while weak reflections on the first layer line corresponding to the periodicity of the *trans*-planar conformation (5.1 Å) appear (Figure 4C,D). At highest deformation ($\epsilon = 500\%$), the 200 reflection at $2\theta = 12^\circ$ almost disappears and fibers in the *trans*-planar disordered mesomorphic form are obtained,^{21,22} as indicated by the presence of the broad equatorial reflection in the range $2\theta = 15\text{--}18^\circ$ centered at $2\theta \approx 17^\circ$ (Figure 4D).

These data indicate that for these low syndiotactic sam-PP samples the ordered *trans*-planar form III does not form by stretching, as instead occurs for highly syndiotactic samples.^{4,6,16,20} Crystals in the helical form

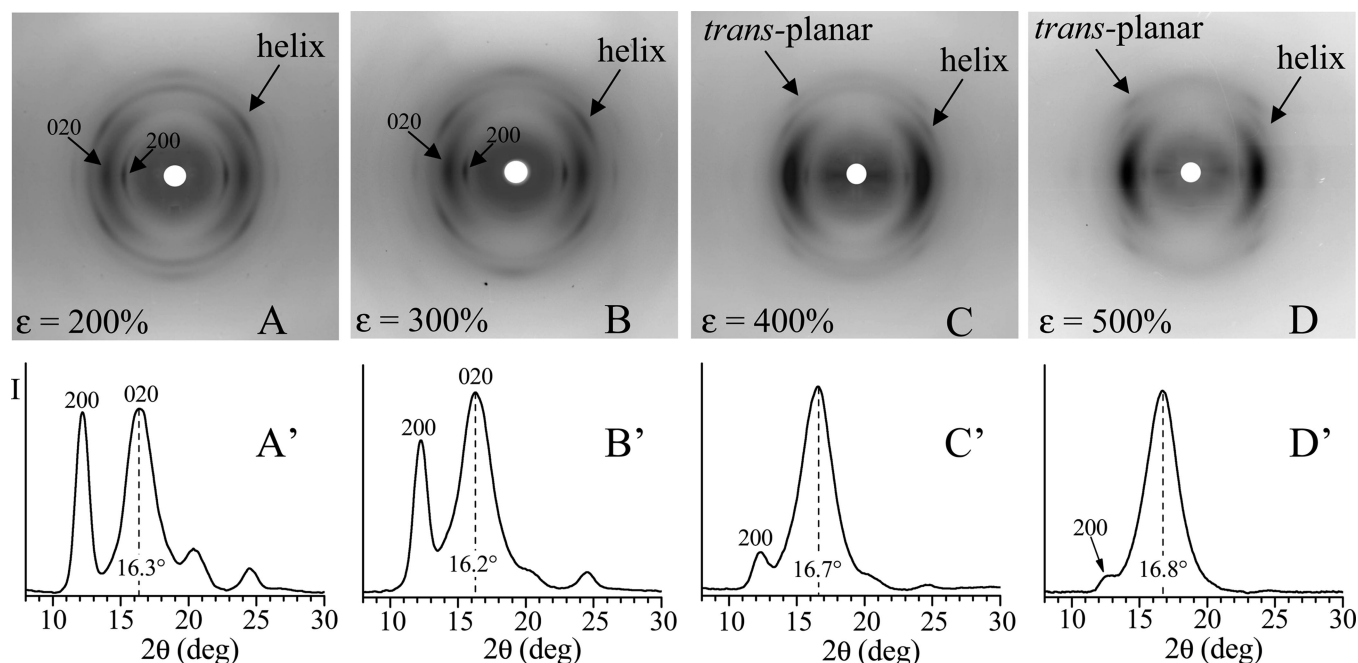


Figure 4. X-ray fiber diffraction patterns, after the subtraction of the amorphous halo (A–D), and corresponding profiles read along the equatorial lines (A'–D'), of fibers of the sample sam-PP1 obtained by stretching at room temperature compression-molded films at values of the strain ϵ of 200% (A), 300% (B), 400% (C), and 500% (D). The 200 and 020 reflections at $2\theta \approx 12^\circ$ and 16° , respectively, typical of the helical form I of s-PP and the 2θ position of the broad reflection of the mesomorphic form at $2\theta = 16\text{--}17^\circ$ are indicated.

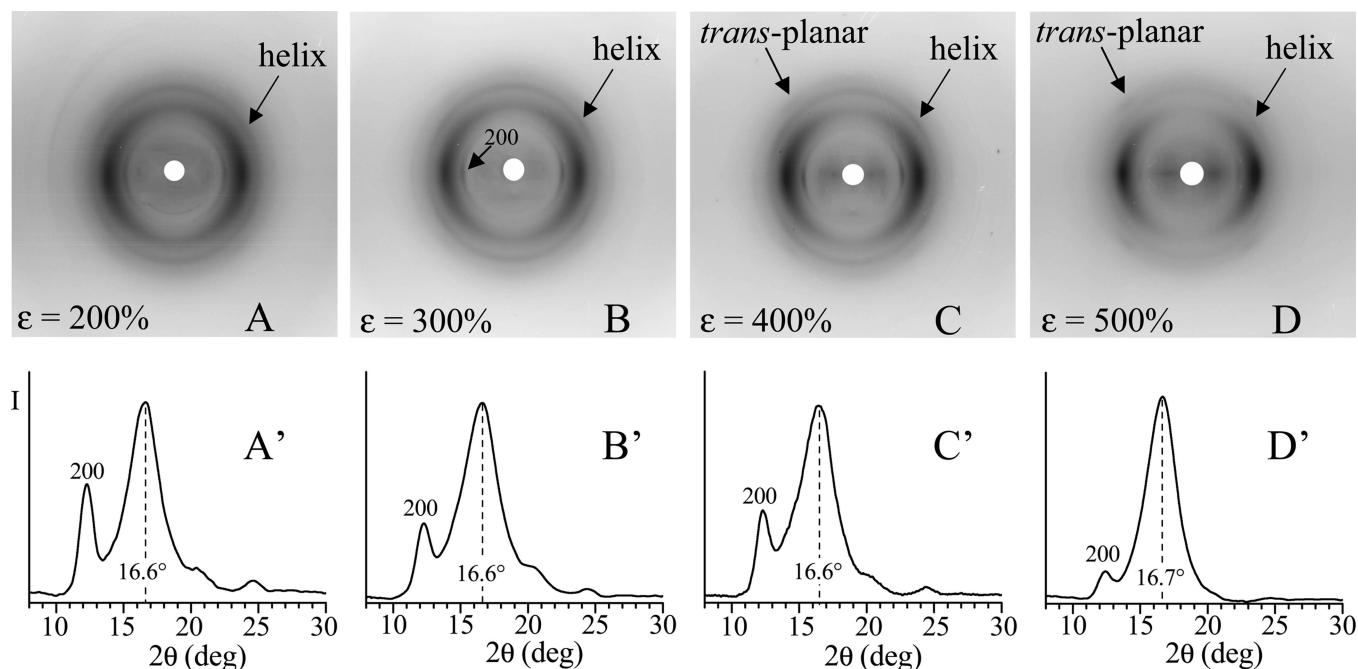


Figure 5. X-ray fiber diffraction patterns, after the subtraction of the amorphous halo (A–D), and corresponding profiles read along the equatorial lines (A'–D'), of fibers of the sample sam-PP3 obtained by stretching at room temperature compression-molded films at values of the strain ϵ of 200% (A), 300% (B), 400% (C), and 500% (D). The 200 reflection at $2\theta \approx 12^\circ$ typical of the helical form I of s-PP and the 2θ position of the broad reflection of the mesomorphic form at $2\theta = 16\text{--}17^\circ$ are indicated.

I, present in the unoriented films, are oriented by stretching at low deformations, and transform into the disordered *trans*-planar mesomorphic form of s-PP by stretching at high deformations. This confirms the data reported in the literature,^{4,6,20} which indicate that the pure *trans*-planar form III can be obtained only for highly stereoregular s-PP samples, with fully syndiotactic pentad *rrrr* content higher than 90%, whereas the stretching of lower stereoregular samples (*[rrrr]* = 75–80%) generally produces mixtures of helical and *trans*-planar forms.^{6,20,23} The presence of a high concentration of defects of stereoregularity prevents the formation of form III probably because these defects are more tolerated in the helical form than in the *trans*-planar form.^{6,7} In the case of the sam-PP samples the very low stereoregularity does not prevent the formation of the *trans*-planar conformation, probably because the low crystallinity and the high molecular weight allow stretching at very high deformation, forming extended chains. However, the high concentration of defects prevents the packing of the *trans*-planar chains in the ordered lattice of form III, and only the disordered mesomorphic form is obtained (Figure 4).

Similar behavior has been observed for samples sam-PP3, sam-PP4, and sam-PP5, which show a slightly lower syndiotacticity (*[rrrr]* = 41–47%, Table 1). As an example, the X-ray fiber diffraction patterns of fibers of the sample sam-PP3, having the highest molecular weight, are reported in Figure 5. It is apparent that, also in this case, the *trans*-planar mesomorphic form is obtained by stretching at high deformation ($\epsilon = 500\%$) (Figure 5D,D'). Remarkable differences with the higher syndiotactic samples sam-PP1 and sam-PP2 (Figure 4) are observed only at low values of the draw ratio. Indeed, for the higher syndiotactic samples sam-PP1 and sam-PP2, the stretching at low values of deformation basically produces orientation of the crystals of the disordered helical form I present in the unstretched film (Figure 4A,B). For the lower syndiotactic samples sam-

PP3, sam-PP4, and sam-PP5, the low intensity of the 200 reflection at $2\theta = 12^\circ$ and the presence of a weak reflection on the first layer line corresponding to the *trans*-planar conformation in the patterns of Figure 5A,A',B,B' indicate that a smaller amount of crystalline phase in the helical form I and a nonnegligible amount of mesomorphic form are present in fibers stretched at low draw ratios. This indicates that a partial transformation of the helical form I, present in the unstretched film, into the *trans*-planar mesomorphic form already occurs at low deformations (Figure 5A,B). Moreover, the stretching at low draw ratios produces low degrees of orientation of the crystals of the helical form (Figure 5A,B). Only at high deformations a well-oriented mesomorphic form is obtained (Figure 5D). The behavior of these three samples is the same regardless of the different molecular weights.

As a matter of fact, the presence of the broad equatorial reflection in the range $2\theta = 15\text{--}18^\circ$ even in the patterns of Figure 4B,B' indicates that a certain amount of *trans*-planar mesomorphic form is obtained already at low deformations also for the higher stereoregular sam-PP1 and sam-PP2 samples.

The X-ray diffraction patterns and the corresponding equatorial profiles of fibers of the sample sam-PP1 stretched at 300% and 500% deformations, kept under tension and after release of the tension, are reported in Figures 6 and 7, respectively.

Very similar diffraction patterns are observed for the sample sam-PP2. In the case of the fiber stretched at 300% strain, which is mainly in the helical form I (Figure 6A), a partial reduction of the orientation of the crystals of the helical form is observed after release of the tension (Figure 6B). Moreover, an increase of the intensity of the 200 reflection at $2\theta = 12^\circ$ is observed after removal of the tension (Figure 6B'). These data indicate that the fiber of Figure 6A is mainly in the helical form I but contains a nonnegligible amount of *trans*-planar mesomorphic form, as also suggested by

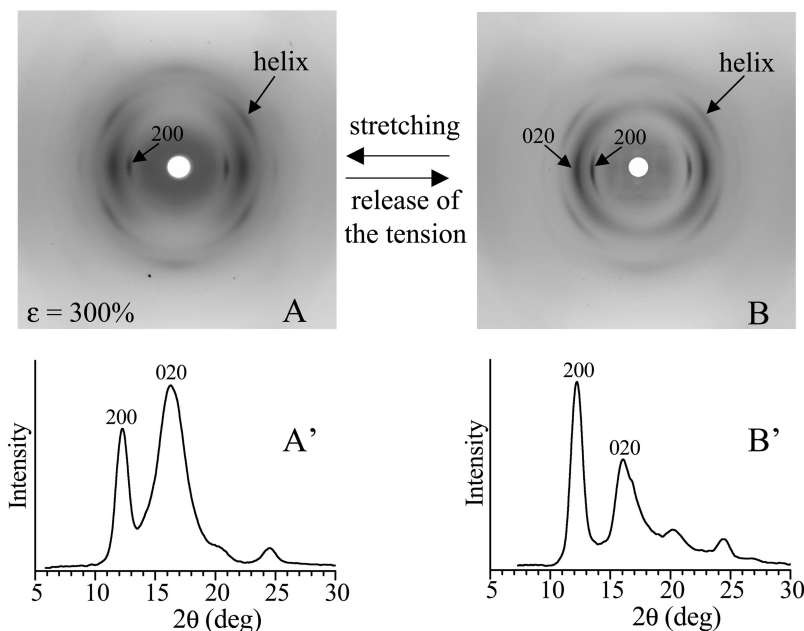


Figure 6. X-ray fiber diffraction patterns, after the subtraction of the amorphous halo (A, B), and corresponding profiles read along the equatorial lines (A', B'), of fibers of the sample sam-PP1 obtained by stretching compression-molded films at 300% elongation, keeping the fiber under tension (A), and after removal of the tension (B). The 200 and 020 reflections at $2\theta = 12^\circ$ and 16° , respectively, typical of the helical form I of s-PP are indicated. The fiber in (A) is in a disordered modification of the helical form I with a small amount of the mesomorphic form, whereas the fiber in (B) is basically in the helical form I.

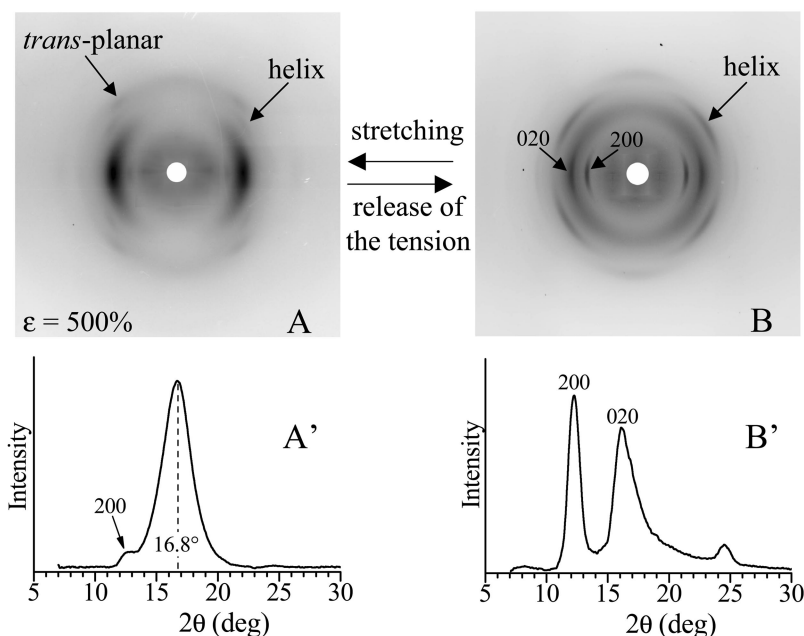


Figure 7. X-ray fiber diffraction patterns, after the subtraction of the amorphous halo (A, B), and corresponding profiles read along the equatorial lines (A', B'), of fibers of the sample sam-PP1 obtained by stretching compression-molded films at 500% elongation, keeping the fiber under tension (A), and after removal of the tension (B). The 200 and 020 reflections at $2\theta = 12^\circ$ and 16° , respectively, typical of the helical form I of s-PP and the 2θ position of the broad reflection of the mesomorphic form at $2\theta = 16.8^\circ$ are indicated. The fibers in (A) is in the *trans*-planar mesomorphic form, whereas the fiber in (B) is basically in the helical form I.

the high intensity of the equatorial peak at $2\theta = 16\text{--}17^\circ$ (Figure 6A'), which is due to the contribution of the 020 reflection of the helical form I and the equatorial reflection of the mesomorphic form. The small amount of the *trans*-planar mesomorphic modification, formed during the stretching at 300% strain, transforms into the helical form I after release of the tension (Figure 6B), and correspondingly, the intensity of the 200 reflection increases, whereas the intensity of the peak at $2\theta = 16^\circ$ decreases (Figure 6B').

As discussed above, for deformations higher than 300% fibers in the pure mesomorphic form are obtained (Figure 7A). Upon release of the tension, the *trans*-planar mesomorphic form transforms into the helical form I (Figure 7B), as indicated by the presence of the 200 and 020 reflections at $2\theta = 12^\circ$ and 16° , typical of the helical form I, in the pattern of Figure 7B,B'. The strong increase of the 200 reflection at $2\theta = 12^\circ$, the reduction of the width of the reflection at $2\theta = 16\text{--}17^\circ$, and the shift of this reflection from $2\theta \approx 17^\circ$ (Figure

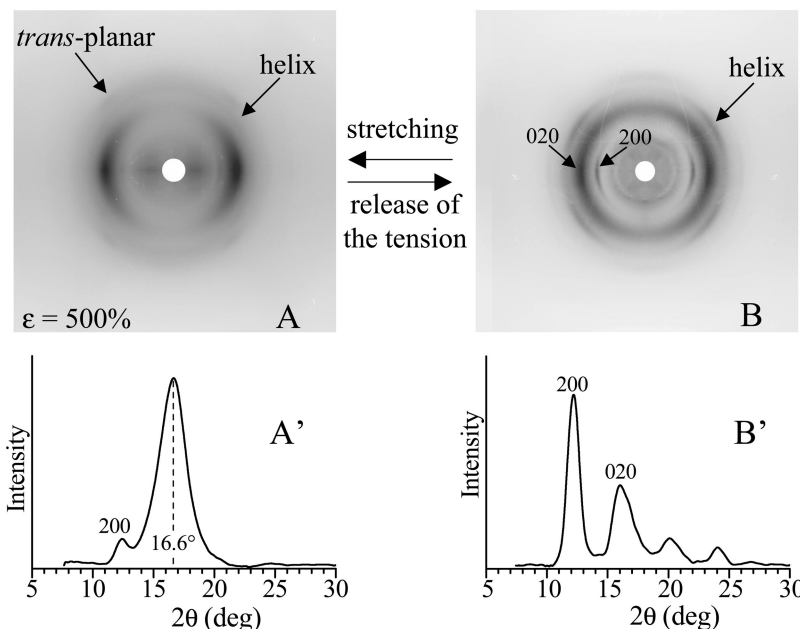


Figure 8. X-ray fiber diffraction patterns, after the subtraction of the amorphous halo (A, B), and corresponding profiles read along the equatorial lines (A', B'), of fibers of the sample sam-PP3 obtained by stretching compression-molded films at 500% elongation, keeping the fiber under tension (A), and after removal of the tension (B). The 200 and 020 reflections at $2\theta = 12^\circ$ and 16° , respectively, typical of the helical form I of s-PP and the 2θ position of the broad reflection of the mesomorphic form at $2\theta = 16.6^\circ$ are indicated. The fiber in (A) is mainly in the *trans*-planar mesomorphic form with a small amount of the helical form, whereas the fiber in (B) is basically in the helical form I.

7A') to $2\theta = 16^\circ$ (Figure 7B') clearly indicate that the mesomorphic form transforms into the helical form I upon release of the tension.

Similar behavior has been observed for the lower syndiotactic samples sam-PP3, sam-PP4, and sam-PP5. The X-ray diffraction patterns of fibers of the sample sam-PP3 stretched at 500% elongation, kept under tension, and after release of the tension are reported in Figure 8. It is apparent that the oriented *trans*-planar mesomorphic form, obtained by stretching (Figure 8A), transforms into the helical form I upon release of the tension, as indicated by the increase of the intensity of the 200 reflection at $2\theta = 12^\circ$ and the shift of the reflection at $2\theta = 16.6^\circ$ to the lower value of $2\theta = 16^\circ$ of form I. Moreover, a remarkable reduction of crystal orientation is observed (Figure 8B).

We recall that for highly syndiotactic polypropylene prepared with the classic C_s -symmetric metallocene catalyst, the stretching of films in the stable helical form I produces the formation of fibers in the *trans*-planar form III,^{4,16} which transforms into the isochiral helical form II of s-PP after removal of the tension.^{6,20} The transition between the *trans*-planar form III and the helical form II is a reversible crystal-crystal transformation, as demonstrated by time-resolved diffraction experiments with synchrotron radiation.³⁴ The data of Figures 6–8 indicate that for the low stereoregular sam-PP samples the isochiral helical form II is never obtained, neither by stretching nor upon release of the tension.

This experimental observation confirms the hypothesis recently reported in the literature that the formation of the isochiral helical form II is strictly related to that of the *trans*-planar form III of s-PP.^{23,35} The isochiral helical form II can be obtained at room temperature only from stretched fibers initially in the *trans*-planar form III upon release of the tension.^{6,20,23} When the formation of the *trans*-planar form III is

prevented, like in the case of the low stereoregular sam-PP samples, the isochiral helical form II does not form anymore. These data are in agreement with the results recently reported on s-PP stretched at different temperatures,²³ or for copolymers of s-PP with 1-butene.³⁵ s-PP fibers stretched at room temperature,^{20,23} or copolymers of s-PP with a small content of 1-butene (1–2 mol %),³⁵ are in the *trans*-planar form III, which transforms into the isochiral helical form II upon release of the tension. With increasing the stretching temperature²³ or the butene content,³⁵ only the antichiral helical form I of s-PP is observed in stretched fibers of the s-PP homopolymer and copolymers, as well as upon release of the tension.^{23,35} The stretching at temperature higher than 60°C ,²³ or the presence of 1-butene units for contents higher than 4 mol %, ³⁵ prevents the formation of the *trans*-planar form III of s-PP by stretching, and the isochiral helical form II does not form any more.^{23,35}

Therefore, anytime the formation of the *trans*-planar form III of s-PP is prevented, like in the presence of butene comonomeric units or by stretching at high temperatures, or for the low stereoregular sam-PP samples, the isochiral helical form II is not observed. The metastable isochiral form II of s-PP can be obtained, at atmospheric pressure, only starting from the *trans*-planar form III by a spontaneous crystal-crystal transformation when the tension in stretched fibers is removed. As discussed in a recent paper³⁶ this transformation, involving a conformational transition from *trans*-planar into a helical conformation, is a cooperative process imposed by steric constraints. The cooperativity induces the formation of helical chains having the same chirality which pack forming the metastable isochiral C-centered form II of s-PP (Figure 1C), even though the antichiral helical form I (Figure 1A) of s-PP is more stable. The results of the sam-PP samples confirm that the helical form II of s-PP can be obtained only through

this cooperative conformational transition. When the *trans*-planar form III is absent, the most stable antichiral form I of s-PP forms in the fiber samples under any conditions.

It is worth noting that sam-PP samples present elastic properties.^{1,37} The small crystalline domains in the amorphous matrix act as physical knots of the elastomeric lattice, preventing the viscous flow of the amorphous chains during stretching. Since the molecular weight is very high, the amorphous chains are highly entangled and connect as tie chains the small crystalline domains. As shown in Figure 3, they are oriented and in extended conformations in the stretched state, and return to the disordered coil conformation when the tension is removed, acting as springs between the crystals. The entropic effect of the conformational transition of the amorphous chains is mainly responsible for the elasticity.^{1,37} A possible crystallization of part of the amorphous component by stretching at high deformation may occur, as suggested by the strain-hardening observed at high deformation in the stress-strain curves of these materials reported in the literature.^{1,37} Finally, the structural analysis has shown that inside the small crystalline domains a reversible polymorphic transition between the disordered helical form I and the mesomorphic *trans*-planar form occurs. Since the crystals are characterized in any case by disordered modifications, they can be more easily plastically deformed. All of these structural and physical properties suggest that these sam-PP samples are novel interesting thermoplastic elastomeric materials.

Conclusion

sam-PP presents a polymorphic behavior different from that observed in highly syndiotactic polypropylene. As-polymerized sam-PP samples are generally amorphous. They do not crystallize by cooling the melt to room temperature but slowly crystallize at room temperature in several days in disordered modifications of form I of s-PP. Disorder in the alternation of right- and left-handed helical chains along the axes of the unit cell and disorder in the stacking of *bc* layers of chains along *a*, implying shifts of *bc* layers of *b/4* along *b*, are present. A low degree of crystallinity, in the range 16–20%, is achieved.

Oriented fibers of the semicrystalline sam-PP samples, stretched at low values of the draw ratio, are mainly in the helical form I. At higher deformations ($\epsilon = 500\%$) the helical form transforms into the *trans*-planar disordered mesomorphic form. For these poorly syndiotactic sam-PP samples the ordered *trans*-planar form III does not form by stretching, as instead occurs for highly syndiotactic samples. This confirms the data reported in the literature^{4,6,20} that the pure *trans*-planar form III can be obtained only for a highly stereoregular s-PP sample. The presence of a high concentration of defects of stereoregularity prevents the formation of form III probably because these defects are more tolerated in the helical form than in the *trans*-planar form.^{6,7} In the case of sam-PP samples the very low stereoregularity does not prevent the formation of the *trans*-planar conformation, probably because the low crystallinity and the high molecular weight allow stretching at very high deformations, forming extended chains. However, the high concentration of defects prevents the packing of the *trans*-planar chains in the ordered lattice of form III, and only the disordered mesomorphic form is obtained.

The *trans*-planar mesomorphic form transforms into the helical form I upon release of the tension in stretched fibers. The isochiral helical form II of s-PP, which can be obtained in fibers of the highly stereoregular s-PP initially in the *trans*-planar form III by removing the tension,^{6,20} is never observed for the low stereoregular sam-PP. These data confirm that the metastable isochiral form II of s-PP can be obtained, at atmospheric pressure and at room temperature, only starting from the *trans*-planar form III by a spontaneous crystal-crystal transformation when the tension in stretched fibers is removed.^{6,20} This transformation, involving a conformational transition from *trans*-planar into a helical conformation, is a cooperative process imposed by steric constraints.³⁶ The cooperativity induces the formation of helical chains having the same chirality which pack forming the metastable isochiral C-centered form II of s-PP, even though the antichiral helical form I of s-PP is more stable.³⁶ The data of the sam-PP samples confirm that the helical form II of s-PP can be obtained only through this cooperative conformational transition. Anytime the formation of the *trans*-planar form III of s-PP is prevented, like for the poorly syndiotactic sam-PP samples, the isochiral helical form II is not observed and the most stable antichiral form I of s-PP is obtained in the relaxed fiber samples.

The poorly syndiotactic polypropylene sam-PP samples present interesting elastomeric behavior due to the presence of small crystalline domains in the amorphous matrix, which act as physical knots of the elastomeric lattice. Since the molecular weight is very high, the amorphous chains are highly entangled and connect as tie chains the small crystalline domains. They are oriented and in extended conformations in the stretched state, and return to the disordered coil conformation when the tension is removed, acting as springs between the crystals.

Acknowledgment. Financial support from Basell Polyolefins (Ferrara, Italy) and from the Ministero dell'Istruzione, dell'Università e della Ricerca (PRIN 2002 and Cluster C26 projects) is gratefully acknowledged. We thank Dr. Luigi Resconi of Basell for providing the polymer samples and for having stimulated this study.

References and Notes

- (1) De Rosa, C.; Auriemma, F.; Ruiz de Ballesteros, O.; Resconi, L.; Fait, A.; Ciaccia, E.; Camurati, I. *J. Am. Chem. Soc.* **2003**, *125*, 10913.
- (2) Grandini, C.; Camurati, I.; Guidotti, S.; Mascellari, N.; Resconi, L.; Nifant'ev, I. E.; Kashulin, I. A.; Ivchenko, P. V.; Mercandelli, P.; Sironi, A. *Organometallics*, submitted for publication.
- (3) Resconi, L.; Guidotti, S.; Baruzzi, G.; Grandini, C.; Nifant'ev, I. E.; Kashulin, I. A.; Ivchenko, P. V. (Basell, Italy). PCT Int. Appl. WO 01/53360, 2001.
- (4) De Rosa, C.; Corradini, P. *Macromolecules* **1993**, *26*, 5711.
- (5) De Rosa, C.; Auriemma, F.; Vinti, V. *Macromolecules* **1997**, *30*, 4137.
- (6) De Rosa, C.; Auriemma, F.; Vinti, V. *Macromolecules* **1998**, *31*, 7430.
- (7) De Rosa, C.; Auriemma, F.; Vinti, V.; Galimberti, M. *Macromolecules* **1998**, *31*, 6206.
- (8) De Rosa, C.; Auriemma, F.; Ruiz de Ballesteros, O. *Polymer* **2001**, *42*, 9729.
- (9) Natta, G.; Corradini, P.; Ganis, P. *Makromol. Chem.* **1960**, *39*, 238.
- (10) Corradini, P.; Natta, G.; Ganis, P.; Temussi, P. A. *J. Polym. Sci., Part C: Polym. Symp.* **1967**, *16*, 2477.
- (11) Natta, G.; Peraldo, M.; Allegra, G. *Makromol. Chem.* **1964**, *75*, 215.

- (12) Lotz, B.; Lovinger, A. J.; Cais, R. E. *Macromolecules* **1988**, *21*, 2375.
- (13) Lovinger, A. J.; Lotz, B.; Davis, D. D. *Polymer* **1990**, *31*, 2253.
- (14) Lovinger, A. J.; Davis, D. D.; Lotz, B. *Macromolecules* **1991**, *24*, 552.
- (15) Lovinger, A. J.; Lotz, B.; Davis, D. D.; Padden, F. J. *Macromolecules* **1993**, *26*, 3494.
- (16) Chatani, Y.; Maruyama, H.; Noguchi, K.; Asanuma, T.; Shiomura, T. *J. Polym. Sci., Part C: Polym. Lett.* **1990**, *28*, 393.
- (17) Chatani, Y.; Maruyama, H.; Asanuma, T.; Shiomura, T. *J. Polym. Sci., Part B: Polym. Phys.* **1991**, *29*, 1649.
- (18) De Rosa, C.; Auriemma, F.; Corradini, P. *Macromolecules* **1996**, *29*, 7452.
- (19) Auriemma, F.; De Rosa, C.; Ruiz de Ballesteros, O.; Vinti, V. *J. Polym. Sci., Part B: Polym. Phys.* **1998**, *36*, 395.
- (20) Auriemma, F.; Ruiz de Ballesteros, O.; De Rosa, C. *Macromolecules* **2001**, *34*, 4485.
- (21) Nakaoki, T.; Ohira, Y.; Hayashi, H.; Horii, F. *Macromolecules* **1998**, *31*, 2705.
- (22) Vittoria, V.; Guadagno, L.; Comotti, A.; Simonutti, R.; Auriemma, F.; De Rosa, C. *Macromolecules* **2000**, *33*, 6200.
- (23) De Rosa, C.; Gargiulo, M. C.; Auriemma, F.; Ruiz de Ballesteros, O.; Razavi, A. *Macromolecules* **2002**, *35*, 9083.
- (24) Rastogi, S.; La Camera, D.; van der Burgt, F.; Terry, A. E.; Cheng, S. Z. D. *Macromolecules* **2001**, *34*, 7730.
- (25) Zhang, J.; Yang, D.; Thierry, A.; Wittmann, J. C.; Lotz, B. *Macromolecules* **2001**, *34*, 6261.
- (26) Auriemma, F.; Born, R.; Spiess, H. W.; De Rosa, C.; Corradini, P. *Macromolecules* **1995**, *28*, 6902.
- (27) Auriemma, F.; Lewis, R. H.; Spiess, H. W.; De Rosa, C. *Macromol. Chem. Phys.* **1995**, *196*, 4011.
- (28) Auriemma, F.; De Rosa, C.; Ruiz de Ballesteros, O.; Corradini, P. *Macromolecules* **1997**, *30*, 6586.
- (29) De Rosa, C.; Auriemma, F.; Vinti, V.; Grassi, A.; Galimberti, M. *Polymer* **1998**, *39*, 6219.
- (30) De Rosa, C.; Auriemma, F.; Talarico, G.; Busico, V.; Caporaso, L.; Capitani, D. *Macromolecules* **2001**, *35*, 1314.
- (31) De Rosa, C.; Auriemma, F.; Fanelli, E.; Talarico, G.; Capitani, D. *Macromolecules* **2003**, *36*, 1850.
- (32) Auriemma, F.; De Rosa, C.; Corradini, P. *Macromolecules* **1993**, *26*, 5719.
- (33) Loos, J.; Hückert, A.; Petermann, J. *Colloid Polym. Sci.* **1996**, *274*, 1006. Loos, J.; Petermann, J.; Waldöfner, A. *Colloid Polym. Sci.* **1997**, *275*, 1088.
- (34) Auriemma, F.; De Rosa, C. *J. Am. Chem. Soc.* **2003**, *125*, 13143. *Macromolecules* **2003**, *36*, 9396.
- (35) De Rosa, C.; Auriemma, F.; Orlando, I.; Talarico, G.; Caporaso, L. *Macromolecules* **2001**, *34*, 1663.
- (36) Lotz, B.; Mathieu, C.; Thierry, A.; Lovinger, A. J.; De Rosa, C.; Ruiz de Ballesteros, O.; Auriemma, F. *Macromolecules* **1998**, *31*, 9253.
- (37) De Rosa, C.; Auriemma, F.; Ruiz de Ballesteros, O. *Macromolecules* **2003**, *36*, 7607.

MA034805D